IMPACT OF INCOMPLETE IONISATION ON MEASUREMENTS OF SHEET RESISTIVITY AND OF CARRIER MOBILITY IN c-SI SOLAR CELLS AT ROOM TEMPERATURE

P.P. Altermatt,[1,2] A. Schenk,[3] B. Schmithüsen[3] and G. Heiser[4]
[1]Institute for Solid-State Physics, University of Hannover, Appelstr. 2, 30167 Hannover, Germany
[2]Insitute for Solar Energy Research Hameln (ISFH), Am Ohrberg 1, 31860 Emmerthal, Germany, www.isfh.de
[3]Integrated Systems Laboratory, ETH-Zentrum, ETHZ, Gloriastrasse 35, 8092 Zurich, Switzerland, schenk@iis.ee.ethz.ch
[4]Computer Science and Engineering, University of NSW, Sydney 2052, Australia, g.heiser@unsw.edu.au

ABSTRACT: When the Fermi level is situated close to the dopant level, the dopant states are noticeably occupied, leading to incomplete ionisation. The free carrier density is then noticeably smaller than the dopant density, although all dopant atoms replace Si atoms and are 'electronically active'. So far, this effect has been mostly neglected in device modelling and optimisation. However, we show that incomplete ionisation is significant at room temperature at dopant densities near 1×10^{18} cm^{-3}, and we quantify the influence of this statistical effect on measurements of sheet resistivity and of carrier mobility – both these parameters affect the design of c-Si solar cells.
Keywords: Modelling, Silicon, Doping

1 INTRODUCTION

A few recent papers propose ways to implement incomplete ionisation (abbreviated as 'ii') in device models [1-3]. All these recent papers conclude that there is an increasing amount of ii with increasing dopant density N_{dop}. However, we show in this work that these conclusions are incompatible with measurements: due to the metal-insulator transition, the dopant level approaches the band edge at high dopant densities, leading to rather complete ionisation. Hence, ii is an important effect only in the N_{dop} range near 10^{18} cm^{-3}, as has been suggested before [4]. However, we show in this paper that ii remains an important effect at room temperature.

2 EXPERIMENTAL FOUNDATION

We first consider phosphorus-doped crystalline silicon at temperatures T below 10 K, since the mechanisms determining the density-of-states (DOS) near the band-edges have been mainly studied in this temperature range.

2.1 The DOS at low dopant densities

When a phosphorus atom replaces a Si atom in the crystal lattice, its outermost electron orbital has a ground state ('impurity state') with an observed energy E_{imp} = -45.5 meV below the conduction band edge E_c, and it is doubly degenerate. There are also seven excited states observed below E_c. However, most of these states are empty at T > 20 K, where we will apply our model, and therefore these states are neglected in our DOS model.

In the following, we consider the properties of the donor states with rising N_{dop}. Assuming random distribution and $N_{dop} < 1\times10^{16}$ cm^{-3}, most neighboring phosphorus atoms are situated far apart, and their bound electron states do not interact with each other. Thus, practically all donor states have the same energy E_{imp}. However, when two phosphorus atoms are randomly situated more closely together than two Bohr radii, their donor states undergo quantum mechanical mixing due to Coulomb interaction. At $N_{dop} > 2\times10^{16}$ cm^{-3}, the number of such randomly occurring phosphorus pairs is large enough to cause the DOS of the donor states to slightly broaden into a donor band D_{imp}.

The higher the N_{dop}, the more phosphorus atoms are randomly situated closer together than two Bohr radii. Eventually, not only pairs are formed, but also groups of various sizes, called donor clusters. At $N_{dop} > 1\times10^{18}$ cm^{-3}, clusters containing three and four phosphorus atoms become more abundant than isolated phosphorus atoms. This has two main effects. Firstly, the DOS broadens significantly, because the donor states within these clusters interact with each other. Secondly, E_{imp} starts to approach the conduction band edge, because the electrons are less strongly bound to the phosphorus cores with growing cluster size.

At 4.2 K, the electrons move rather freely within their clusters. However, these electrons do not contribute to a macroscopic DC conductivity σ, since they cannot move from cluster to cluster within the donor band. Only when N_{dop} reaches the critical value [5] of N_{crit} = 3.74×10^{18} cm^{-3}, can a sufficient number of clusters connect with each other so that DC conductivity on a macroscopic scale is enabled in the donor band. The transition in the behavior of σ happens within a very small range of N_{dop}, and is called the Mott, metal-insulator (M-I), or the metal-nonmetal (MNM) transition.

In Fig. 1, we re-interpret the photoluminescence (PL) data of Bergersen et al. [6]. These authors measured the PL spectrum of Si:P at various excitation powers at 4.2 K. At low powers (shown as crosses), the PL spectrum shows the donor band, because radiation is mainly caused by electrons that recombine from the donor to the valence band. At high powers, the PL spectrum is dominated by electrons that recombine from the conduction band (shown as open symbols). One may think at first that E_{imp} can be derived from such PL measurements by simply comparing the PL peaks at low and high excitation powers. However, this is not the case because, with increasing power, a growing number of free carriers are injected into the sample, causing an increasing amount of band gap narrowing ΔE_g. Hence, these two peaks are shifted in different amounts towards lower energies. We are able to calculate ΔE_g at both levels of excitation power, using the model of Ref. [7]. From Figure 1 we determine E_{imp} = -15 meV and a donor band-width of approximately 30 meV at N_{crit}. This is one of the main outcomes of this paper, showing that the clusters fuse on a macroscopic scale while the donor band is separate from the conduction band. The donor band just touches the conduction band at N_{crit}. Is this an arbitrary coincidence? No, for the following reasons. The electron gas theory predicts that entirely free carriers have a parabolic en-

ergy-momentum (E-k) relation and hence a DOS $\sim E^{1/2}$. Bound electrons have a flat E-k relation, which is curved more and more with a decreasing amount of localisation [8]; this causes D_{imp} to widen with increasing N_{dop}. The electrons that become free on a macroscopic scale at N_{crit} do not contribute to D_{imp}; they are contained in the DOS of the conduction band D_c, and make the transition when parts of D_{imp} exceed E=0.

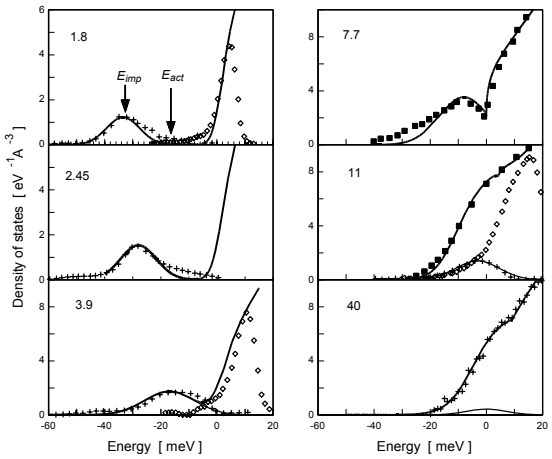

Figure 1: The measured Si:P photoluminescence intensity [6] (arbitrary units) at low injection power (crosses) and at high injection power (open symbols), and the DOS derived from tunneling measurements [11,12] (squares), at various phosphorus densities ($\times 10^{18}$) and at 4.2 K. The solid lines are our parameterisation of the DOS.

Our findings stay in contrast to what is widely accepted in the silicon community and written in textbooks, namely that the donor band merges completely with the conduction band at N_{crit}. A more detailed analysis will be published elsewhere.

2.2 The DOS above the M-I transition

It is apparent from Figure 1 that E_{imp} approaches the conduction band edge only gradually at dopant densities above N_{crit}. This is expected from theoretical investigations showing that the donor clusters have various sizes. Above N_{crit}, mainly small clusters remain isolated from the other clusters, and their electrons are rather strongly bound to the phosphorus cores, leading to $E_{imp} < E_c$.

To derive a parameterisation of the DOS, the knowledge of E_{imp} alone is insufficient; we need to estimate as well which fraction of electrons is still bound to these isolated clusters. We should keep in mind that D_{imp} in Figure 1 contains only the electron states bound to clusters, and not the free ones. This estimate is expressed by the factor b in Equation (1). With growing N_{dop}, there are fewer and fewer isolated clusters, causing b to decline. We obtain a lower limit of b from magnetic susceptibility and specific heat measurements [9,10]. From them, the density of electrons having localised magnetic momentum, n_{lm}, can be derived. The ratio n_{lm}/N_{dop} is depicted in Figure 2 as crosses. This is only a lower limit, because (i) only localised states with an odd occupation number carry a local magnetic moment, and (ii) many electrons in clusters have a sufficiently large localisation length such that their magnetic moment does not appear as localised. However, two important features become apparent from Figure 2: firstly, n_{lm}/N_{dop} decreases most rapidly with rising N_{dop} at the M-I transition; and secondly, there exists a considerable number of localised electrons up to $N_{dop} \approx 1\times10^{19}$ cm^{-3}.

In addition, we can obtain limits to b from considerations other than localised magnetic moments: depending on b, the overall DOS (of the impurity plus the conduction band) may or may not have a local minimum. For example, the DOS in Fig. 1 at $N_{dop} = 7.7\times10^{18}$ cm^{-3} has a local minimum, while the DOS at $N_{dop} = 1.1\times10^{19}$ cm^{-3} does not (unless b would be substantially increased). PL measurements are not feasible to confirm or deny such a local minimum because they are obtained using two different measurements at two different illumination intensities (crosses and open symbols in Fig. 1). Fortunately, there are also DOS data available, obtained by current-voltage (I-V) measurements of n-Si/Sn tunnel structures [11,12]. These measurements show that the local minimum in the overall DOS disappears near or below $N_{dop} = 1\times10^{19}$ cm^{-3}. We therefore determine the upper limit of b by calculating the DOS such that no local minimum occurs at the above dopant density. The results are shown as triangles in Figure 2. As it is an upper limit, it lies above the squares, except near $N_{dop} = 1\times10^{20}$ cm^{-3}, where more localised magnetic momenta seem to arise due to band tailing than due to the impurity band.

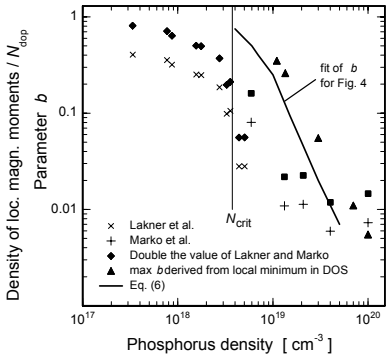

Figure 2: The density of localized magnetic moments n_{lm}, divided by N_{dop}, as derived from magnetic susceptibility and specific heat measurements (crosses) in Si:P. The two-fold amount (squares) is a lower limit for the density of localized states in the impurity band. The upper limit is derived from DOS measurements (triangles). Parameter b (solid line) is adjusted by fitting the calculated amount of ii to experimental values shown in Fig. 4.

These upper and lower limits generally lie far apart, and no precise adjustment of b is possible on these grounds. However, b strongly influences the amount of ii. Therefore, we will adjust b by fitting the calculated ii to experimental values.

We obtain information about the DOS at still higher N_{dop} by means of the far-infrared reflectance spectra [13]. They can be accurately reproduced by the Drude model at $N_{dop} = 7.4\times10^{19}$ cm^{-3} by assuming that the effective (density-of-states) electron mass m_{dc} is essentially the same as at low N_{dop}. There are additional measurements that indicate that m_{dc} depends only very weakly on N_{dop} up to $N_{dop} \approx 1\times10^{20}$ cm^{-3}. This implies that the DOS at such high dopant densities is essentially parabolic (apart from the band tail effects).

We show in a separate paper that the DOS does not change significantly when going from 4.2K to 300K.

3 PARAMETERISATION OF THE DOS

We approximate the donor band D_{imp}, shown in Fig. 1, by a Gaussian distribution function:

$$D_{imp} = \frac{N_{dop} b}{\sqrt{2\pi}\delta} \exp\left[\frac{-(E - E_{imp})^2}{2\delta^2}\right]. \qquad (1)$$

We call δ the half-width of the donor DOS, and b is the fraction of electrons bound to isolated clusters.

From Figure 1, we extract E_{imp} and the activation energy E_{act} (explained in Fig. 1), and compare these values in Figure 3 with measurements from the literature. Because we can closely approximate D_{imp} in Figure 1 by a Gaussian (i.e. symmetrical) profile, the difference between E_{imp} and E_{act} is approximately half the width of the donor band. Considering this, our data coincides with the literature data, and we parameterise E_{imp} with the following logistical equation:

$$E_{imp} = \frac{E_{imp,low}}{1 + \left(N_{dop} / N_{imp}\right)^c}, \qquad (2)$$

using $N_{imp} = 3\times10^{18}$ cm^{-3} and $c = 2$. From Figure 3, it becomes apparent that E_{act} starts to change at $N_{dop} \approx 1\times10^{17}$ cm^{-3} due to band broadening, and that E_{imp} stays rather constant up to $N_{dop} \approx 1\times10^{18}$ cm^{-3}. At higher N_{dop}, both parameters change rather abruptly. E_{act} becomes zero at the M-I transition, while E_{imp} approaches zero (i.e. E_c) gradually above $N_{dop} \approx 1\times10^{19}$ cm^{-3}. E_{imp} cannot move into the conduction band because the principal reason for its variation is screening.

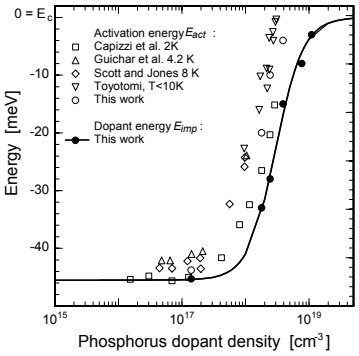

Figure 3: The energy of the the donor band peak E_{imp} in Si:P (filled circles) and the activation energy of the donor band E_{act} (empty circles), as derived from Fig. 1. The other symbols show E_{act} values, obtained from various measurement techniques. The solid line is our parameterisation using Eq. (2).

We extract the half-width of the impurity band, δ, by fitting the PL measurements in Figure 1 with Eq. (1), and use the empirical expression

$$\delta = r N_{dop}^{1/2} (1 - e^{-s/N_{dop}}) \qquad (3)$$

with $r = 4.2\times10^{-12}$ eVcm$^{-3/2}$ and $s = 10^{19}$ cm^{-3}. With growing N_{dop} beyond N_{crit}, δ decreases because smaller and smaller clusters stay isolated and contribute to D_{imp}.

The only remaining parameter to be adjusted is b, which quantifies the fraction of electrons that remains bound to dopant clusters above N_{crit}. We already obtained a lower and upper limit in Fig. 2. As b strongly influences the amount of ii, we adjust b by fitting the calculated ii to experimental values as follows.

Because the free electron density n equals the ionised phosphorus density N^+_{dop} up to about 400 K, ii is the ratio N^+_{dop}/N^0_{dop}, where N^0_{dop} is the neutral (non-ionised) dopant density. We obtain the amount of ii by self-consistently solving the following three equations at a given N_{dop}:

$$N^0_{dop} = \int_{-\infty}^{E_c} D_{imp}(E) f_D(E, E_F) dE,$$

$$N^+_{dop} = \int_{E_c}^{\infty} [D_{imp}(E) + D_c(E)] f(E, E_F) dE, \qquad (4a\text{-}c)$$

$$N_{dop} = N^0_{dop} + N^+_{dop}.$$

The unknown parameters in this equation system are N^0_{dop}, N^+_{dop} and the Fermi energy E_F. The occupation probability of the impurity states,

$$f_D = 1/(1 + g e^{(E - E_F)/kT}), \qquad (5)$$

differs from the Fermi-Dirac function f, by the degeneracy factor g, because each localised state in the impurity band can be occupied by only a single electron due to the Coulomb interaction.

We require measurements of n/N_{dop} to verify our calculations of ii. We found that the most precise way to obtain this is to compare the published data of conductivity mobility μ_{cond} with the data of Hall mobility μ_H (details will be published somewhere else). The direct measurements in Figure 4 were obtained by measuring μ_H and μ_{cond} in the same samples. The indirect measurements are μ_H measurements that we related to an empirical parameterisation of μ_{cond}, as is explained in a separate paper.

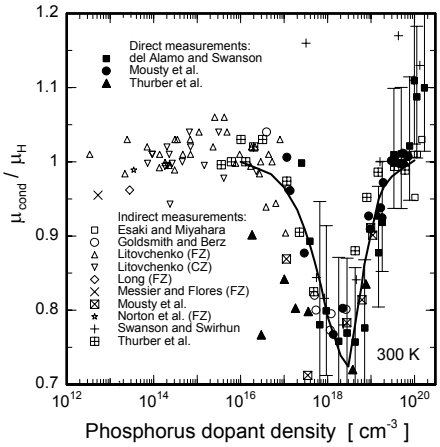

Figure 4: The fraction between measured conductivity mobility and Hall mobility (symbols) in Si:P, reflecting incomplete ionisation, which is compared with our calculations (lines).

Our calculations with Eqs. (4a-c) fit the experimental data very well within the experimental precision if we adjust b with

$$b = \frac{1}{1 + (N_{dop} / N_b)^d}, \qquad (6)$$

using $N_b = 6\times10^{18}$ cm^{-3} and $d = 2.3$ (shown in Fig. 2 as line). This implies that at the M-I transition, only about 5% of electrons in the clusters become free. We haven't found experimental verification of this in the literature.

Figure 4 shows that, at 300 K, up to 25% of electrons

are non-ionised – a result that challenges common beliefs that ii can be neglected at room temperature.

The situation is similar in boron-doped silicon, as shown in Fig. 5. The list of parameters, used in Eqs. (1)-(6), is as follows:

Parameter	Si:P	Si:B	Si:As
$E_{imp,low}$ [meV]	45.5	44.39	53.7
N_{imp} [cm^{-3}]	3×10^{18}	1.7×10^{18}	4×10^{18}
c	2	1.4	1.5
r [eVcm$^{-3/2}$]	4.2×10^{-12}	4.2×10^{-12}	4.2×10^{-12}
s [cm^{-3}]	10^{19}	10^{19}	10^{19}
N_b [cm^{-3}]	6×10^{18}	6×10^{18}	1.4×10^{19}
d	2.3	2.4	3
g	1/2	1/4	1/2

4 IMPACT ON FREE-CARRIER MOBILITY

Regardless of how mobility μ is measured, it has to be related to either N_{dop}, the sample resistivity ρ, or the carrier density n present during the experiment. This is where ii comes into play in mobility measurements.

In the PV community, μ is usually parameterised as a function of N_{dop} (and not of carrier density) using Thurber's equation [14], or an extension of Thurber's to higher N_{dop} given by Masetti [15], which was extended to temperatures other than 300K by Klaassen [16]. All three parameterisations assume that ii was substantially smaller than derived from measurements here. This is so because Thurber's work on ii was not based on measurements. An underestimation of ii causes an underestimation of μ. Our aim is to correct this.

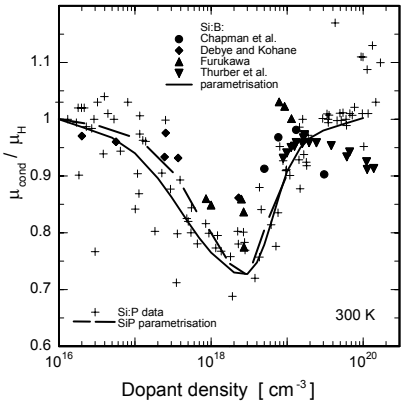

Figure 5: The fraction between measured conductivity mobility and Hall mobility (symbols) in Si:B, reflecting incomplete ionisation, which is compared with our calculations (lines).

In order to include μ correctly in device simulations, one needs to consider the following three issues: firstly, was the parameterisation of μ obtained using data as a function of N_{dop} or n? Was ii considered/relevant when referring to N_{dop} or n? Secondly, was ii taken into account when determining the magnitude of the μ values? Thirdly, does the simulation need to neglect or include ii to be consistent with the μ values? In practically all device simulations, at least one of these three issues is addresses incorrectly.

In order to achieve a consistent procedure, we suggest two different options:

a) the simulation neglects ii; then, the μ parameterisation needs to neglect ii as well; or
b) the simulation includes ii; then, the μ parameterisation must be obtained with regarding ii as well.

Figure 6 shows μ values that are corrected from literature values by totally neglecting ii (crosses and empty symbols), or by taking our amount of ii into account (filled symbols). For example at N_{dop} = 1×10^{18} cm^{-3}, μ rises from 277 to 372, which is a rise by 35%! Hence, μ is the least precise parameter used in device simulations.

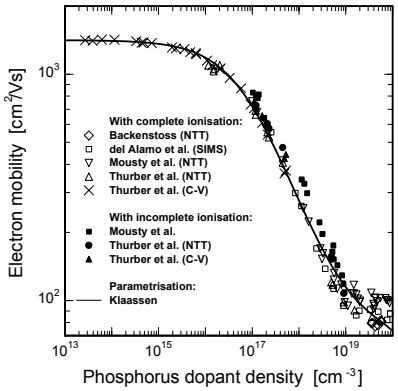

Figure 6: The mobility of majority electrons as a function of phosphorus dopant density, either obtained by neglecting ii or by taking ii, as derived here, into account.

4 IMPACT ON SHEET RESISTANCE

Because μ (usually as a function of N_{dop}) is used in measurements/calculations of the sheet resistance ρ of a diffused layer, ii comes into play as well. Taking the two mobility dependences of Figure 6, a high-efficiency emitter with N_{peak} = 5×10^{18} cm^{-3} and depth d = 1 μm of the Gaussian profile yields ρ = 200 or 153 Ω/sq., respectively. Care must be taken whether the dopant profile is determined via secondary ion mass spectroscopy (SIMS) or via stripping Hall effect measurements, because the former determines N_{dop} while the latter determines n.

[1] H. Watanabe, J. Appl. Phys. 90 (2001) 1600.
[2] G. Xiao et al., Microel. Reliability 39 (1999) 1299.
[3] Y. Yue and J. J. Liou, Sol.-St. El. 39 (1996) 318.
[4] G.L. Pearson, J. Bardeen, Phys. Rev. 75 (1949) 865.
[5] T. F. Rosenbaum et al., Phys. Rev. B27 (1983) 7509.
[6] B. Bergersen et al., Phys. Rev. B14 (1976) 1633.
[7] A. Schenk, J. Appl. Phys. 84 (1998) 3684.
[8] J. Monecke et al., Phys. Rev. B47 (1993) 9377.
[9] M. Lakner et al., Phys. Rev. B50 (1994) 17064.
[10] J. R. Marko et al, Phys. Rev. B10 (1974) 2448.
[11] K. P. Abdurakhmanov et al., Soviet Physics of Semiconductors 10 (1976) 393.
[12] J. Nishizawa and M. Kimura, Jap. J. Appl. Phys. 14 (1975) 1529.
[13] A. Gaymann et al., Phys. Rev. Let. 71 (1993) 3681.
[14] W.R. Thurber, J. Electron. Mat. 9 (1980) 551.
[15] Masetti et al., IEEE Trans. El. Dev. 30 (1983) 764.
[16] D.B.M. Klaassen, Solid-St. El. 35 (1992) 953.